10Be exposure ages and paleoenvironmental significance of rock glaciers in the Western Tatra Mts., Western Carpathians

Tereza Dlabáčková, Zbyněk Engel, Tomáš Uxa, Team Aster

^{10}Be exposure ages for rock glaciers in the Western Tatra Mts., Western Carpathians

Tereza Dlabáčková[a,b,*], Zbyněk Engel[a], Tomáš Uxa[c], Régis Braucher[d], Aster Team[d]

[a]Faculty of Science, Charles University, Prague, Czech Republic
[b]Czech Geological Survey, Prague, Czech Republic
[c]Institute of Geophysics, Czech Academy of Sciences, Prague, Czech Republic
[d]CEREGE CNRS Aix Marseille Univ., IRD, INRAE, Collége de France, Aix-en-Provence, France

*Corresponding author at: Faculty of Science, Charles University, Albertov 6, Prague 2, 128 00, Czech Republic. E-mail address: tereza.dlabackova@natur.cuni.cz (T. Dlabáčková)
Aster Team: G. Aumître, F. Zaidi, K. Keddadouche

Abstract

Relict rock glaciers are well-preserved features of high-elevated valleys in the Western Tatra Mts., Western Carpathians, but their chronology remained poorly constrained with numerical dating methods. We present the first robust set of ^{10}Be exposure ages for eight rock glaciers with front elevation of 1376–1819 m asl. The results suggest that the rock glaciers stabilized throughout the Weichselian Lateglacial from ~16.5 ka to 11 ka. This timing is consistent with the period of rock glacier stabilisation in European mountain regions but it extends the age span previously determined for rock glaciers in the Tatra Mts. There are differences between north- and south-facing valleys in the elevation and time of the stabilization of the rock glaciers, which were probably caused by contrasts in potential incoming solar radiation that affected the retreat of former glaciers and the subsequent formation of the rock glaciers. The initiation altitude of ~1610 and ~1830 m asl determined for the oldest and youngest dated rock glaciers is generally consistent with previous estimates of the glacier equilibrium line altitude during the Greenland Stadials 2.1 and 1, respectively. However, the lower limit of the rock glaciers is well above regional paleopermafrost features from the same periods, which suggests that rock glaciers may underestimate past permafrost extents and temperature declines disputing their regional validity for paleoenvironmental reconstructions.

***Keywords*:** Quaternary, Lateglacial, Cosmogenic isotopes, Paleoclimatology, Permafrost, Europe

1 Introduction

Rock glaciers are thick lobate- or tongue-shaped masses of angular debris and ice that move slowly down high mountain slopes due to the deformation of the internal ice, which also causes the formation of a typical surface relief of rock glaciers consisting of transverse and longitudinal ridges and furrows (Barsch, 1996; French, 2017; Ballantyne, 2018). The source of the material is debris from adjacent talus slopes for so-called talus rock glaciers or moraine deposits covering valley floors for so-called debris rock glaciers (Barsch, 1996; Ballantyne, 2018). Active rock glaciers are supposed to form and move in regions with low precipitation and mean annual air temperature (MAAT) <−2 °C (Barsch, 1996; Humlum, 1998). At higher temperatures, topographic constraints or limited debris supply, their activity ceases and they turn into inactive rock glaciers, and if the ice core (~permafrost) melts completely they become relict rock glaciers (Barsch, 1996; Kääb, 2013). Consequently, the individual types of rock glaciers tend to be

located at elevation zones, which correspond to specific temperature conditions. Elevation of rock glacier fronts has thus been widely used as a proxy indicator for present and past lower limit of discontinuous permafrost or for past climatic conditions in which the rock glaciers formed and were active (Frauenfelder et al., 2001). Relict rock glaciers are valuable in that they can provide a proxy record of past environmental conditions where other natural archives, such as lake sediments, may be incomplete. Determining the age of relict rock glaciers is thus important for understanding the postglacial evolution of mountain relief, especially in the Tatra Mts., where this period of landscape development has not yet been sufficiently explored.

The age of rock glaciers has formerly been determined using several methods of relative dating such as measuring the surface weathering of rock boulders with the Schmidt hammer (Frauenfelder et al., 2005; Kellerer-Pirklbauer, 2008a, 2008b; Kłapyta, 2011, 2013; Zasadni and Kłapyta, 2016, Zasadni et al., 2020), weathering rind thickness (Laustela et al., 2003), lichenometry (Haeberli et al., 1979; Hamilton and Whalley, 1995; Nicholas and Butler, 1996; Refsnider and Brugger, 2007) or alternatively by photogrammetric and geodetic measurements of the rock glacier flow (Kääb et al., 1998; Vespremeanu-Stroe et al., 2012). However, recent decades have seen an expansion in numerical dating methods using radionuclides ^{14}C preserved in organic remnants buried by rock glaciers (e.g. Scapozza et al., 2010; Krainer et al., 2015) and cosmogenic radionuclides ^{36}Cl (e.g. Palacios et al., 2015; Moran et al., 2016; Fernandez-Fernandez et al., 2020) and ^{10}Be (e.g. Ivy-Ochs et al., 2009; Steinemann et al., 2020; Zasadni et al., 2020) in surface boulders on rock glaciers. A combination of relative and numerical dating methods has also widely been used for so-called Schmidt hammer exposure-age dating (Rode and Kellerer-Pirklbauer, 2012; Matthews et al., 2013; Matthews and Winkler, 2022).

Cosmogenic exposure dating of rock glaciers in Europe has so far been carried out in the Iberian Peninsula (Palacios et al., 2015, 2016; Rodriguez-Rodriguez et al., 2016, 2017; Andrés et al., 2018; Garcia-Ruiz et al., 2020; Santoz-Gonzales et al.,2022), the Alps (Ivy-Ochs et al., 2006, 2009; Hippolyte et al., 2009; Böhlert et al., 2011; Moran et al., 2016; Steinemann et al., 2020; Charton et al., 2021), Tröllaskagi Peninsula, Iceland (Fernandez-Fernandez et al., 2020; Palacios et al., 2021), Øyberget, Norway (Linge et al., 2020), Cairngorm Mts., Great Britain (Ballantyne et al., 2009), or the Romanian Carpathians (Vasile et al., 2022). Most authors attributed the exposure age of rock glaciers to a period of their stabilization, which started no earlier than in the Greenland Stadial 2.1a (GS-2.1a) (Rodriguez-Rodriguez et al., 2016; Steinemann et al., 2020; Ballantyne et al., 2009) and continued until the mid-Holocene at the latest (Palacios et al., 2016; Palacios et al., 2021).

However, dating of rock glaciers in some other European regions, such as the Tatra Mts., Western Carpathians, has been limited. The age of rock glaciers in the Tatra Mts. was initially deduced based on paleoclimatic considerations and relative dating methods. Kotarba (1992) claimed based on paleoclimatic reconstructions that rock glaciers in the Tatra Mts. formed during the Greenland Stadial 1 (GS-1) (~Younger Dryas). Several authors extended the age span of rock glaciers in the Tatra Mts. using the Schmidt hammer test to the entire Lateglacial (Kłapyta, 2011, 2013; Zasadni and Kłapyta 2016; Zasadni et al., 2020), but these estimates have not yet been fully confirmed by numerical dating. For the Western Tatra Mts., there is only one study providing exposure ages of ~13 and ~12 ka for the stabilization of rock glaciers (Engel et al., 2017). In the High Tatra Mts., Zasadni et al. (2020) dated the final phase of stabilization of the highest-elevated rock glaciers in cirques to the end of the GS-1 to early

Holocene. However, numerical ages for the stabilization of lower-elevated and probably older rock glaciers are still lacking.

The main objective of this study is to determine the chronology of the stabilization of rock glaciers in the Western Tatra Mts. using ^{10}Be exposure dating. We hypothesize that the lowest-lying rock glaciers at ~1400 m asl could represent the period of early deglaciation after the local last glacial maximum (LGM) and those in high-lying cirques at ~1800 m asl could be from the beginning of the Holocene. We also compare the rock glacier chronology with similar investigations on rock glaciers as well as with other local and regional paleoenvironmental records.

2 Study area

The Western Tatra Mts. (the highest peak Bystrá at 2248 m asl) together with the High Tatra Mts. (2654 m asl) and the Belianske Tatra Mts. (2152 m asl) represent the northernmost part of the Carpathian arch, situated on the Slovak-Polish border (Fig. 1). The main ridge of the Western Tatra Mts. stretches in a roughly west-east direction for 42 km (the entire mountain chain is ~70 km long), while the maximum width of the mountain range is 16 km.

The Western Tatra Mts. are mainly composed of crystalline rocks of the Paleozoic age (State Geological Institute of Dionýz Štúr, 2013). Most of the mountain range consists of igneous rocks (granitoids), but the southern and northern parts are built of metamorphic rocks (micaschists, gneisses). In the outer areas of the mountain range, especially in the north, the crystalline rocks are overlain by Mesozoic sedimentary rocks (limestones, sandstones) (State Geological Institute of Dionýz Štúr, 2013; Králíková et al., 2014). The Western Tatra Mts. are bounded in the south by the sub-Tatra fault, along which the southern crests were uplifted to slightly higher elevations than the northern ones. The largest uplift accelerated from the end of the Late Miocene to the Pleistocene (Baumgart-Kotarba and Kráľ, 2002; Králíková et al., 2014; Jacko et al., 2021; Vitovič et al., 2021) and has continued into the postglacial period as documented by post-LGM fault scarps (Pánek et al., 2020). The Western Tatra Mts. are ~300 m lower compared to the High Tatra Mts., which is due to the asymmetrical rise of the individual blocks of the mountain range in the west-east direction (Baumgart-Kotarba and Kráľ, 2002; Jurewicz, 2007; Králíková et al., 2014).

The Tatra Mts. were glaciated several times during the cold phases of the Pleistocene as indicate sequences of glacial and glaciofluvial sediments in front of the mountains (Lindner et al., 2003). The last glacial episode culminated during the local LGM, which terminated before ~18 ka in the Western Tatra Mts. (Engel et al., 2017). During the subsequent Lateglacial period, at least two still-stands or re-advances occurred in north-facing valleys (Makos et al., 2016; Engel et al., 2017). Nowadays, glaciers are no longer present (Gądek, 2014), as the climatic snowline is estimated at 2500–2600 m asl on the northern slopes and at 2700–2800 m asl on the southern ones (Zasadni and Kłapyta, 2009); only firn-ice patches or perennial snowfields persist (Gądek, 2014). The lower limit of discontinuous permafrost is estimated at 1930 ± 150 m asl, depending on the local relief (Dobiński, 2005).

The Western Tatra Mts. represent a significant barrier to the air masses flowing from the northwest to the southeast, causing climatic differences between the northern and southern slopes (Niedzwiedz, 1992). The MAAT in the northern and southern foothills was approximately 6 °C and 8 °C in 1991–2010, respectively (Niedzwiedz et al., 2015; Żmudzka et al., 2015). The ridge part experienced the MAAT of

approximately −2 °C to 0 °C in the same period (Żmudzka et al., 2015), and the mean annual precipitation was >1800 mm in 1981–2010 (Ustrnul et al., 2015).

The study area is situated in the central part of the Western Tatra Mts. on the northern and southern slope of the main ridge (Figs. 1 and 2). The ridge area is built mainly of biotite granodiorite-tonalite to muscovite-biotite granodiorite (High Tatra Type) but porphyritic granitoid and leucogranite prevail around the Volovec and Rákoň peaks (Nemčok et al., 1994). The bedrock is overlain by extensive talus cones on the lower parts of the slopes and foothills, which are dissected by numerous debris flows (Kłapyta, 2015; Dlabáčková and Engel, 2022). The valley floors are filled with rock glaciers or glacigenic sediments (Kłapyta, 2009, 2011, 2013, 2015; Engel et al., 2017; Uxa and Mida, 2017, Zasadni et al., 2022). The Smutna and Spálena valleys on the north side of the main ridge are among the best developed glacial landscapes within the Western Tatra Mts. (Engel et al., 2017). However, deeply incised cirques also form the upper part of the Žiarska and Jamnícka valleys (Fig. 2).

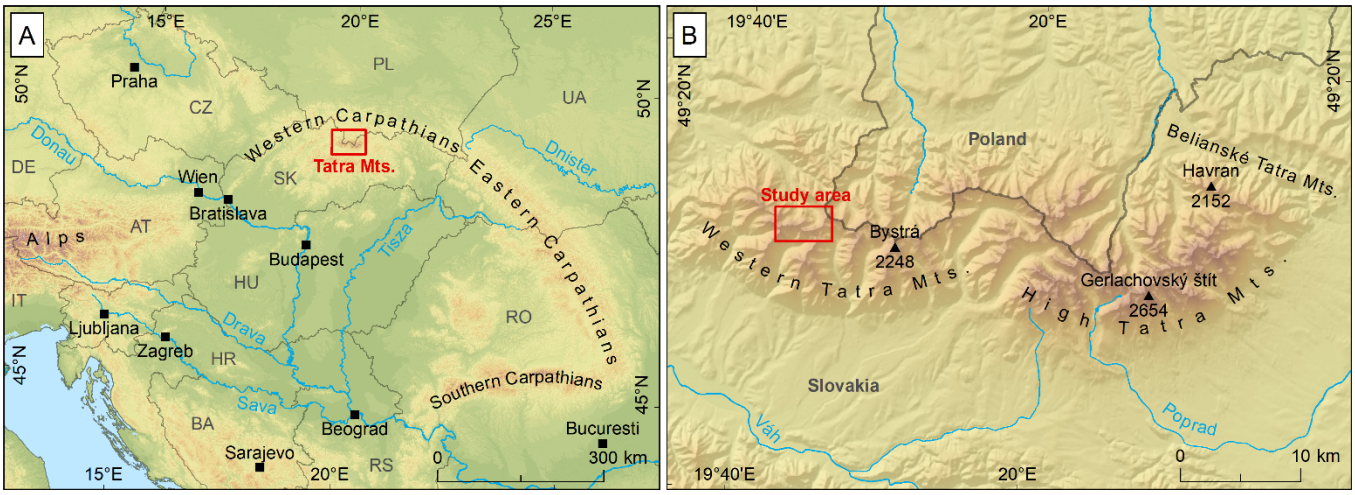

Fig. 1. Location of (A) the Tatra Mts. within the Carpathians and (B) the study area in the Tatra Mts.

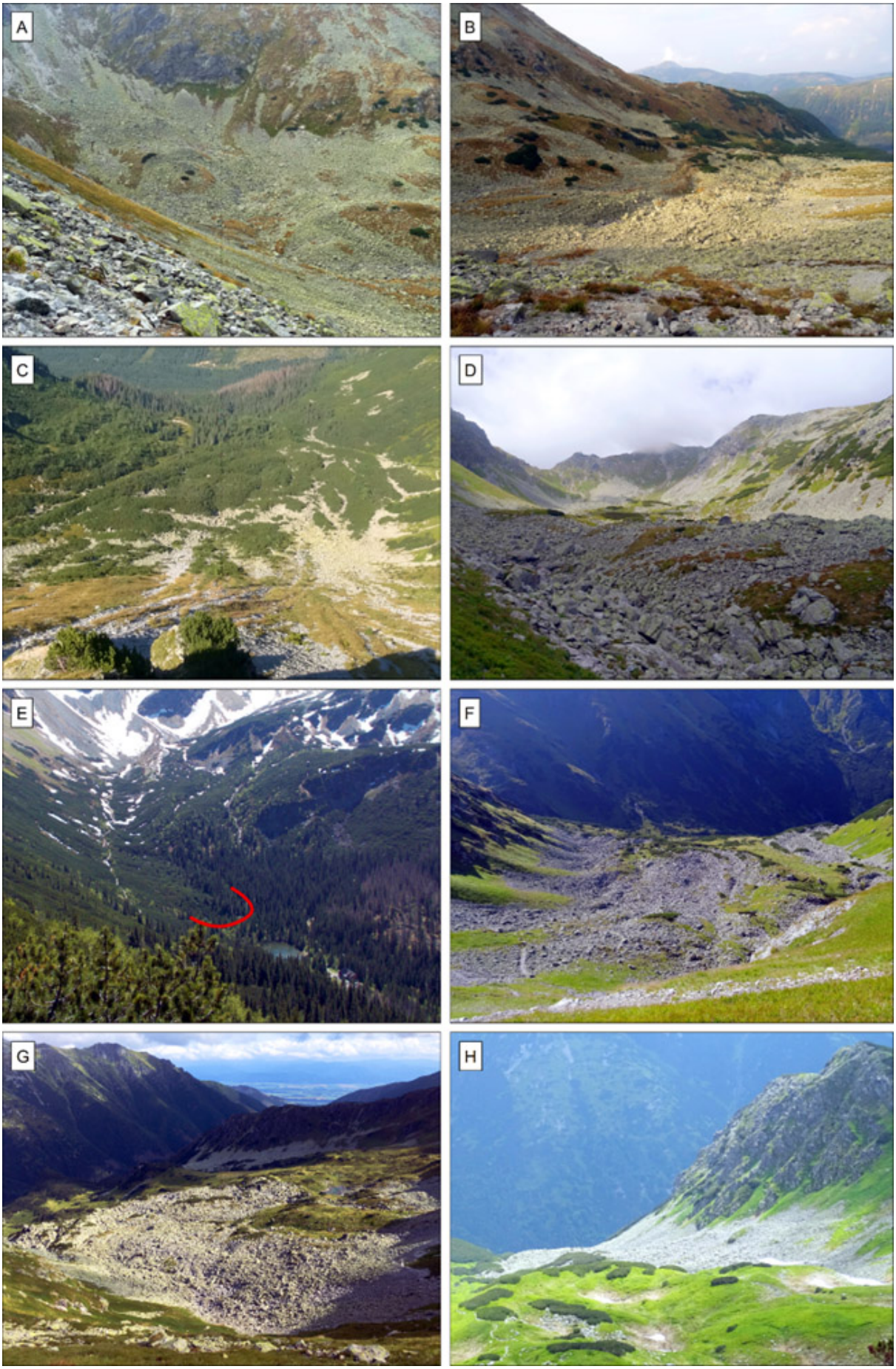

Fig. 2. Rock glaciers selected for exposure dating in the Spálena (A) upper, (B) middle, and (C) lower valley; (D) Smutna valley; (E) Roháčska valley; (F) Žiarska valley; Jamnícka (G) north and (H) south valley.

3 Methods

3.1 Rock glacier selection and characteristics

Eight rock glaciers spanning from low-lying valley bottoms to high-lying cirques oriented north and south of the main ridge of the Western Tatra Mts. were selected for exposure dating. The diagnostic features used to identify the rock glaciers were their distinctive morphology with steep fronts, transverse and longitudinal ridges and furrows, which indicate former downslope movement of the debris material (Barsch, 1996; RGIK, 2022).

The identification of the rock glaciers was based on LiDAR digital elevation model (DEM) with a horizontal resolution of 1 m (The Geodesy, Cartography and Cadastre Authority of the Slovak Republic) as well as orthophotos with a resolution of 0.2 m (Geodetic and Cartographic Institute Bratislava, National Forest Centre). All the delineated rock glaciers were checked and modified by field mapping in 2019−2021, the existing inventory of rock glaciers of the Tatra Mts. (Uxa and Mida, 2017) and previous studies from the study area (Nemčok and Mahr, 1974; Kłapyta, 2009, 2011, 2013, 2015; Engel et al., 2017). For each delineated rock glacier, elevation, flowline length and orientation, width, area, surface slope, front height and slope, and potential incoming solar radiation were determined from the DEM in accordance with conventional procedures (e.g. Barsch, 1996; Kellerer-Pirklbauer et al., 2012; Colucci et al., 2016). The rock glaciers were classified based on length-to-width ratio as lobate- (<1) and tongue-shaped (>1; Barsch, 1996). Their activity was assessed based on the presence of vegetation and soil cover (Barsch, 1996; Kääb, 2013) and the mean slope of the front (≤35° for relict rock glaciers; Haeberli, 1985; Barsch, 1996; Ballantyne, 2018).

The MAAT at the front of the rock glaciers was derived using a multiple linear regression based on the data collected during the period 1951–1970 at twenty weather stations (703–2635 m asl) in the Tatra Mts. (Niedzwiedz, 1992) as follows:

$$\mathrm{MAAT} = \beta_0 + \beta_1 x + \beta_2 y + \beta_3 z, \quad (1)$$

where x (°) is the longitude, y (°) is the latitude, z (m) is the elevation, β_0 (47.3913 °C) is the regression intercept, and β_1 (0.8751 °C·°lon^{-1}), β_2 (−1.1335 °C·°lat^{-1}) and β_3 (−0.0047 °C·m^{-1}) is the longitudinal, latitudinal, and elevational air temperature gradient, respectively. The regression relationship explains 95 % of the variability in MAAT and yields a mean absolute error of 0.44 °C. Additionally, it perfectly fits MAAT from the period 1981–2010 at the Kasprowy Wierch (1991 m asl), which is the closest high-elevated weather station with recent air temperature records available.

Since rock glaciers actively form at MAAT <−2 °C (Barsch, 1996; Kääb, 2013), the difference between this temperature threshold and the present MAAT at the front of the rock glaciers was used to estimate the minimum temperature decline when the rock glaciers stabilized (Frauenfelder et al., 2001). The corresponding minimum decrease of the lower limit of discontinuous permafrost was estimated from the elevation difference between the front of the rock glaciers and the present level of the −2 °C mean annual isotherm (~present lower limit of discontinuous permafrost) derived from Eq. (1) rearranged as follows:

$$z_{\mathrm{MAAT}=-2\,^{\circ}\mathrm{C}} = \frac{\mathrm{MAAT}-\beta_0-\beta_1 x-\beta_2 y}{\beta_3}, \quad (2)$$

which yields the present lower limit of discontinuous permafrost at ~2320 m asl.

3.2 Rock glacier boulder sampling

A total of 34 rock samples were collected for exposure dating of the eight rock glaciers. Three to six boulders were sampled at each rock glacier to minimize the impact of choosing a boulder with a complex exposure history (Denn et al., 2018). We selected only flat-topped boulders higher than 1 m with no signs of erosion that were located on low-angled transverse ridges near the front of the rock glaciers. Samples were collected from the top surface of the boulders with a hammer and chisel. Sample locations and elevations were recorded using a handheld GPS receiver with ~2 m horizontal accuracy. The locations are shown in Fig. 3 and description of the sampled boulders is given in Table A.1.

3.3 Sample treatment and ^{10}Be age calculations

The samples were crushed, sieved and cleaned with a mixture of HCl and H_2SiF_6. The extraction method for ^{10}Be ($T_{1/2}$ = 1.387 ± 0.017 Ma; Chmeleff et al., 2010; Korschinek et al., 2010) involves isolation and purification of quartz and elimination of atmospheric ^{10}Be. A weighed amount (~0.1 g) of a 3025 ppm solution of ^{9}Be was added to the decontaminated quartz. Beryllium was subsequently separated from the solution by successive anionic and cationic resin extraction and precipitation. The final precipitates were dried and heated at 800 °C to obtain BeO, and finally mixed with niobium powder prior to the measurements, which were performed at the French Accelerator Mass Spectrometry (AMS) National Facility ASTER (CEREGE, Aix-en-Provence).

The beryllium data were calibrated directly against the STD-11 beryllium standard using a ^{10}Be/^{9}Be ratio of 1.191 ± 0.013·10^{-11} (Braucher et al., 2015). Age uncertainties include an external AMS uncertainty of 0.5 %, blank correction and 1σ uncertainties (Arnold et al., 2010). The ^{10}Be/^{9}Be measured blank ratio associated with the samples is 3.618·10^{-15}. A density of 2.5 g·cm^{-3} was used for all samples. A sea-level, high-latitude spallation production of 4.01 ± 0.18 at g^{-1}·a^{-1} (Borchers et al., 2016) was used and scaled for latitude and elevation using Stone (2000) scaling scheme. The surface production rates were also corrected for the local slope and topographic shielding due to the surrounding terrain (Dunne et al., 1999). Shielding from snow was estimated according to Gosse and Phillips (2001) using an average snow density of 0.3 g·cm^{-3} and an estimated mean thickness and duration of snow cover at the sample sites. These values were determined based on the data collected during the period 1960/61–1989/90 at nine weather stations (725−1991 m asl) in the Tatra Mts. (Kočický, 1996).

^{10}Be concentrations were modelled using the equation:

$$C_{(x,\varepsilon,t)} = \frac{P_{spall.}}{\frac{\varepsilon}{\Lambda_n}+\lambda}.e^{-\frac{x}{\Lambda_n}}\left[1-\exp\left\{-t\left(\frac{\varepsilon}{\Lambda_n}+\lambda\right)\right\}\right] + \frac{\mathrm{P}_{\mu}}{\frac{\varepsilon}{\Lambda_\mu}+\lambda}.e^{-\frac{x}{\Lambda_\mu}}\left[1-\exp\left\{-t\left(\frac{\varepsilon}{\Lambda_\mu}+\lambda\right)\right\}\right],$$

(2)

where $C_{(x,\ \varepsilon,\ t)}$ is the nuclide concentration as a function of depth x (g·cm^{-2}), the denudation rate ε (g·cm^{-2}·a^{-1}), and the exposure time t (a). P_{spall} and P_{μ} (at·g^{-1}·a^{-1}) are the relative production rates due to neutrons and muons, respectively. Λ_n and Λ_{μ} (g·cm^{-2}) are the effective apparent attenuation lengths for neutrons and muons, respectively, and λ (a^{-1}) is the radioactive decay constant. The muon scheme follows Braucher et al. (2011).

Individual ages are reported with an external error of 1σ, which accounts for both measurement uncertainties, including uncertainties associated with AMS counting statistics, chemical blank measurements and AMS internal error (0.5 %), as well as uncertainties in the reference nuclide production rate for spallation and the nuclide production rate by muons (Balco et al., 2008). At each site, a weighted mean exposure age was calculated and reported with a weighted mean standard deviation.

The chi-squared (χ^2) test was used to examine the distribution of exposure ages at each site (Ward and Wilson, 1978). The 95% critical value for χ^2 with n–1 degrees of freedom was calculated for each site and compared with the theoretical value given by a χ^2 table. If the calculated value was less than the theoretical value, all ages were used to calculate the mean exposure age. However, if the site did not pass this test, the ages with the largest calculated χ^2 value were successively excluded until the distribution passed the χ^2 test (Dunai, 2010). Additionally, the reduced χ^2 statistic (χ^2_R) and the standard deviation to arithmetic mean exposure age ratio was used to approximate the scatter in the data and classify the age groups as well-, moderately- or poorly-clustered (class A, B, and C, respectively) following Blomdin et al. (2016).

4 Results

4.1 Distribution and morphology of rock glaciers

The eight dated rock glaciers occur at an elevation of 1376−1893 m asl (mean 1693 m asl) and their fronts extend to 1376−1819 m asl (mean 1613 m asl) where the present-day MAAT attains 0.2–2.4 °C (mean 1.2 °C, Table 1). Their average length is 591 m, while the average width is 188 m and they occupy an average area of 0.1 km^2. The mean height of the rock glacier fronts is 21 m. Most of the rock glaciers are oriented to the east (four) and northeast (two). The lowermost rock glaciers have predominantly a northeast and northwest orientation. On the contrary, the highest-elevated rock glaciers face east and south. All the rock glaciers are tongue-shaped because the length-to-width ratio is 1.2 (northern Jamnícka valley) to 8.6 (middle Spálena valley, Table 1). Similarly, all the rock glaciers are considered relict because they are prominently covered with vegetation and the mean slope of the fronts ranges between 28° (Roháčska valley) and 33° (Smutna valley).

Table 1. Morphometric and climate characteristics of the dated rock glaciers in the Western Tatra Mts.

Rock glacier	Aspect	Minimum elevation (m asl)	Maximum elevation (m asl)	Mean elevation (m asl)	Length of the flowline (m)	Mean width (m)	Area (km^2)	Mean slope (°)	Mean slope of the front (°)	Mean height of the front (m)	Potential incoming solar radiation ($W \cdot m^{-2}$)	MAAT at the front (°C)
Jamnícka-North	E	1745	1845	1798	448	360	0.13	17	32	26	155	0.6
Jamnícka-South	E	1632	1839	1757	852	129	0.11	17	31	20	147	1.2
Roháčska	NW	1376	1429	1404	240	192	0.03	18	28	9	129	2.4
Smutna	E	1564	1824	1713	1106	169	0.16	18	33	20	132	1.5
Spálena-Lower	NE	1465	1568	1513	366	255	0.09	17	32	18	130	1.9
Spálena-Middle	NE	1594	1824	1728	1032	120	0.11	19	31	24	135	1.3
Spálena-Upper	E	1819	1893	1856	192	128	0.02	24	30	22	138	0.2
Žiarska	S	1706	1855	1778	493	154	0.08	21	32	32	167	0.8

4.2 ^{10}Be exposure ages

The ^{10}Be exposure ages obtained for the collected samples are given in Table 2 and Fig. 3. Five out of 34 exposure ages are identified as outliers and excluded from the dataset based on the results of the χ^2 test (Table 3). Two outlier ages obtained for the samples SPA-4 and SPA-6 are excluded from the dataset obtained in the lower part of the Spálena valley. The remaining four exposure ages range from 17.8 ± 0.7 ka to 14.5 ± 1.2 ka and yield a weighted mean exposure age of 16.6 ± 0.6 ka. At the Spálena valley head closure, the sample SPA-9 with an exposure age of 20.9 ± 1.3 ka is identified as an outlier and excluded from the mean exposure age calculation for the site. The remaining two samples yield a weighted mean exposure age of 13.6 ± 0.7 ka. Apparently young age of 12.4 ± 0.4 ka was obtained for the sample ZIA-2 collected in the Žiarska valley where four other exposure ages give a weighted mean exposure age of 14.9 ± 0.4 ka. The last outlier age of the sample JAM-9 is identified in the set of samples from the southern rock glacier in the Jamnícka valley. The remaining three exposure ages range from 11.1 ± 0.6 ka to 13.0 ± 0.6 ka and give a weighted mean exposure age of 12.2 ± 0.5 ka.

Table 2. ^{10}Be surface exposure ages for the samples collected at the rock glaciers in the Western Tatra Mts. Samples with outlier exposure ages are shown in italics.

Rock glacier	Sample	Latitude (°N)	Longitude (°W)	Elevation (m asl)	Thickness (cm)	Shielding correction	Production rate (at·g^{-1}·a^{-1})	^{10}Be concentration (at·g^{-1})	^{10}Be age (k
Jamnícka-North	JAM-1	49.195247	19.757970	1779	4	0.87821	16.151	237 398 ± 7280	14.504 ± 0
	JAM-2	49.195336	19.758028	1789	2	0.87412	14.542	188 788 ± 8328	15.583 ± 0
	JAM-3	49.195574	19.757766	1791	4	0.86828	14.667	188 000 ± 10 620	13.199 ± 0
	JAM-4	49.195509	19.757790	1785	3	0.86535	14.616	162 611 ± 9220	13.548 ± 0
	JAM-5	49.194880	19.756940	1793	2	0.86777	14.626	230 485 ± 9388	14.676 ± 0
Jamnícka-South	JAM-6	49.191861	19.763420	1659	3	0.87835	12.159	198 833 ± 7044	12.952 ± 0
	JAM-7	49.191783	19.763369	1680	4	0.87662	12.097	192 945 ± 10 085	12.787 ± 0
	JAM-8	49.191676	19.763368	1680	4	0.87674	12.070	217 075 ± 15 633	11.094 ± 0
	JAM-9	*49.192111*	*19.763369*	*1677*	*2*	*0.86417*	*11.879*	*178 379 ± 10 843*	*15.732 ± 0*
Roháčska	ROH-1	49.211154	19.749687	1418	3	0.89488	15.637	203 643 ± 6779	16.318 ± 0
	ROH-2	49.211242	19.749856	1414	5	0.89314	15.566	177 125 ± 5734	15.910 ± 0
	ROH-3	49.211612	19.749911	1412	4	0.89581	15.983	193 222 ± 6376	18.233 ± 1
	ROH-4	49.211602	19.749830	1409	6	0.89470	16.010	181 683 ± 5805	15.454 ± 0
Smutna	SMU-1	49.200121	19.741379	1724	4	0.86548	15.741	240 364 ± 7635	12.997 ± 0
	SMU-2	49.200201	19.741316	1738	5	0.87012	18.163	224 922 ± 6970	11.351 ± 0
	SMU-3	49.200249	19.740301	1752	4	0.85715	15.554	210 529 ± 6489	12.063 ± 0
	SMU-4	49.200228	19.740171	1756	5	0.86625	15.731	233 125 ± 8078	11.321 ± 0

Spálena-Lower	SPA-1	49.207499	19.725761	1495	3	0.91427	13.982	219 421 ± 9441	16.038 ± 0
	SPA-2	49.207453	19.726210	1519	5	0.91246	14.228	239 711 ± 9068	17.496 ± 0
	SPA-3	49.207574	19.725881	1530	4	0.91069	14.334	202 145 ± 16 491	14.520 ± 1
	SPA-4	*49.209057*	*19.728034*	*1488*	*4*	*0.91526*	*13.922*	*9 556 ± 1294*	*0.704 ± 0.*
	SPA-5	49.209283	19.727911	1487	4	0.91646	13.930	240 855 ± 9728	17.817 ± 0
	SPA-6	*49.209300*	*19.727963*	*1490*	*4*	*0.91646*	*13.962*	*149 855 ± 8403*	*11.041 ± 0*
Spálena-Middle	SPA-10	49.203861	19.714079	1753	5	0.89513	16.680	287 144 ± 16 600	17.888 ± 1
	SPA-11	49.203905	19.714053	1752	3	0.89513	16.667	337 747 ± 23 703	20.747 ± 1
	SPA-12	49.204510	19.715366	1730	5	0.89806	16.436	260 480 ± 9998	16.461 ± 0
Spálena-Upper	SPA-7	49.202105	19.708552	1867	3	0.88088	18.090	244 564 ± 9158	13.820 ± 0
	SPA-8	49.202283	19.708459	1870	3	0.87811	17.909	233 403 ± 9086	13.320 ± 0
	SPA-9	*49.202324*	*19.708682*	*1865*	*4*	*0.88008*	*17.884*	*361 949 ± 22 357*	*20.887 ± 1*
Žiarska	ZlA-1	49.192925	19.735390	1778	6	0.86864	15.587	258 651 ± 8015	15.247 ± 0
	ZlA-2	*49.192764*	*19.735595*	*1779*	*5*	*0.88302*	*16.072*	*233 477 ± 7263*	*12.365 ± 0*
	ZlA-3	49.192787	19.736714	1775	4	0.88102	16.155	252 077 ± 8434	13.508 ± 0
	ZlA-4	49.192514	19.736823	1776	7	0.87666	16.099	212 898 ± 6604	14.795 ± 0
	ZlA-5	49.192598	19.736127	1774	7	0.88071	16.101	218 539 ± 6740	16.573 ± 0

Table 3. ^{10}Be surface exposure ages for the sampled rock glaciers in the Western Tatra Mts.

Rock glacier	Number of samples / sample code	Theoretical χ^2	χ^2	χ^2_R	SD to arithmetic mean exposure age (%)	Age clustering (class)*	Uncertainty-weighted Mean Age ± Uncertainty (ka)	Arithmetic Mean Age ± Uncertainty (ka)
Jamnícka-North	5/ JAM-1 to JAM-5	9.49	5.02	1.3	7	A	14.19 ± 0.38	14.30 ± 0.43
Jamnícka-South	3/ JAM-6 to JAM-8	5.99	2.88	1.4	8	A	12.22 ± 0.51	12.28 ± 0.59
Roháčska	4/ ROH-1 to ROH -4	7.81	2.18	0.7	7	A	16.27 ± 0.60	16.48 ± 0.61
Smutna	4/ SMU-1 to SMU-4	7.81	3.46	1.2	7	A	11.85 ± 0.35	11.93 ± 0.39
Spálena-Lower	4/ SPA-1 to SPA-3, SPA-5	7.81	3.67	1.2	9	A	16.58 ± 0.64	16.47 ± 0.76
Spálena-Middle	3/ SPA-10 to SPA-12	5.99	4.29	2.1	12	B	17.71 ± 0.83	18.37 ± 1.26
Spálena-Upper	2/ SPA-7 to SPA-8	3.84	0.13	0.1	3	A	13.56 ± 0.68	13.57 ± 0.25
Žiarska	4/ ZIA-1, ZIA-3 to ZIA-5	7.81	6.89	2.3	8	B	14.87 ± 0.44	15.03 ± 0.63

* The degree of scatter in ages according to the method of Blomdin et al. (2016)

The dispersion of the exposure ages is rather limited for the rock glaciers in the Roháčska and Smutna valleys (Fig. 3). The four ages obtained in the Roháčska valley are well-clustered between 18.2 ± 1.3 ka and 15.5 ± 0.9 ka, yielding a weighted mean age of 16.3 ± 0.6 ka. Similarly, ages obtained for four samples collected in the Smutna valley are well-clustered between 13.0 ± 0.4 ka and 11.3 ± 0.4 ka, giving a weighted mean age of 11.9 ± 0.4 ka. Well-clustered exposure ages were also obtained for five samples

collected from the northern rock glacier in the Jamnícka valley. These ages range from 15.6 ± 0.5 ka to 13.2 ± 0.4 ka and give a weighted mean exposure age of 14.2 ± 0.4 ka. The three exposure ages obtained for the rock glacier in the middle part of the Spálena valley are moderately-clustered between 20.8 ± 1.5 ka and 16.5 ± 0.6 ka, with a weighted mean age of 17.7 ± 0.8 ka.

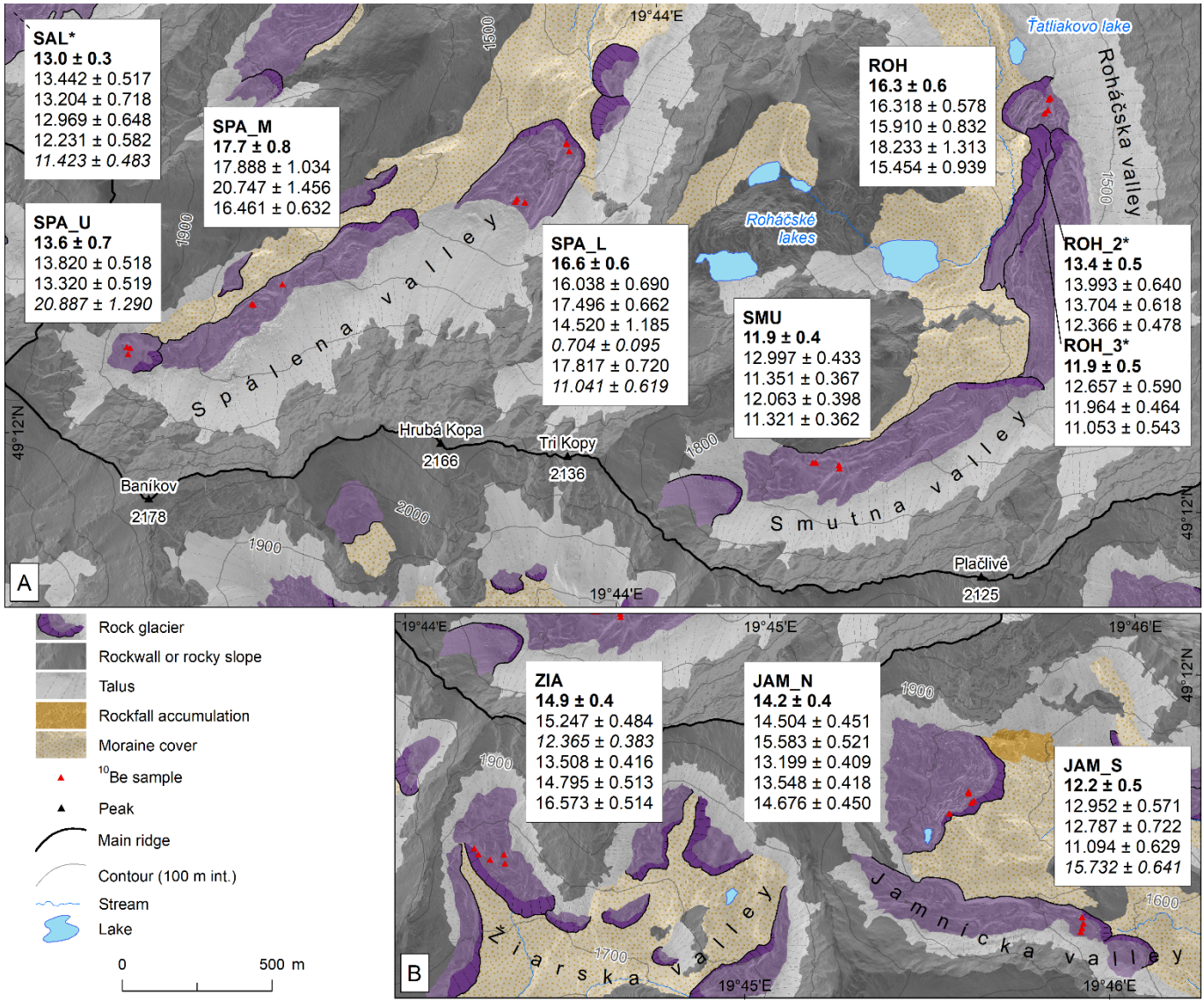

Fig. 3. ^{10}Be exposure ages for the sampled boulders and weighted mean exposure ages (bold) for the dated rock glaciers in the Western Tatra Mts. Italics indicates exposure ages removed from the dataset based on the χ^2 test. Asterisks represent dates published by Engel et al. (2017).

5 Discussion

5.1 Age of rock glaciers

The dated rock glaciers in cirques, middle sections of troughs, and their lower portions above the transition to main valleys represent a complete set of locations where these landforms were found in the Western Tatra Mts. (Uxa and Mida, 2017). The mean elevation of their fronts is only ~30 m lower compared to that reported for all rock glaciers in the Western Tatra Mts. and the dated rock glacier in

the Roháčska valley belongs to the lowermost in the mountain range (Uxa and Mida, 2017). Consequently, we believe that the dated rock glaciers are representative of the whole Western Tatra Mts.

The cosmogenic nuclide ages imply that rock glaciers in the Western Tatra Mts. started to form after the retreat of local glaciers from their LGM positions. The absence of outlier ages in the sample set from the oldest dated rock glacier in the middle Spálena valley suggests that this feature formed after ~18 ka. However, moderately clustered ages indicate movements of individual sampled boulders implying that this rock glacier was ice-cored and active until ~16.5 ka. At that time, glaciers in cirques and tributary valleys were separated from the glacier in the main trough as evidenced by exposure ages reported for the Roháčské lakes area (Engel et al., 2017). The coincident uncertainty-weighted mean ages obtained for the rock glaciers in the lower Spálena (16.6 ± 0.6 ka) and Roháčska (16.3 ± 0.6 ka) valleys suggest that these forms probably evolved from the material of retreating glaciers during the GS-2.1a (17.5 to 14.7 ka; Rasmussen et al., 2014). Later rock glacier stabilization cannot be excluded at the lower Spálena site based on the presence of younger ages in the dataset.

The mean ages calculated for the rock glaciers in the Žiarska, northern Jamnícka, and upper Spálena valleys fall in the Lateglacial interstadial GI-1 (14.7 to 12.9 ka; Rasmussen et al., 2014). Paleoenvironmental proxies in peat and lake sediments indicate continental climate throughout this period with relatively warm summer months until 12.9 ka (Obidowicz, 1996; Rybníčková and Rybníček, 2006). Older mean ages (14.9 ± 0.4 and 14.2 ± 0.4 ka) obtained for the rock glaciers in the southern mountain flank may be attributed to earlier glacier retreat due to the higher potential incoming solar radiation and temperature compared to the upper Spálena rock glacier (13.6 ± 0.7 ka) at higher-elevated site with NE aspect (Table 1). The youngest exposure ages obtained for these rock glaciers indicate their final stabilization within relatively short period (13.5 to 13.2 ka) at the end of the interstadial.

The dated rock glaciers in the southern Jamnícka and Smutna valleys have an eastern orientation similarly to the northern Jamnícka rock glacier, but their surface is shaded by the adjacent mountain ridges as evidenced by the lower beam radiation (Table 1). As a result, glacier snouts melted slowly, and the successive rock glaciers formed as late as in the GS-1 (12.2 ± 0.5 and 11.9 ± 0.4 ka). The youngest exposure ages retrieved for the southern Jamnícka site, as well as a pair of almost identical youngest ages collected in the Smutna valley (Fig. 3) suggest that the rock glaciers at these sites became inactive around 11.3 ± 0.4 ka. This timing coincides with the mean exposure age of 11.1 ± 0.9 ka retrieved for high-elevated rock glaciers in the SW part of the High Tatra Mts. but predates the final stabilization of these landforms around 10.4 ka (Zasadni et al., 2020).

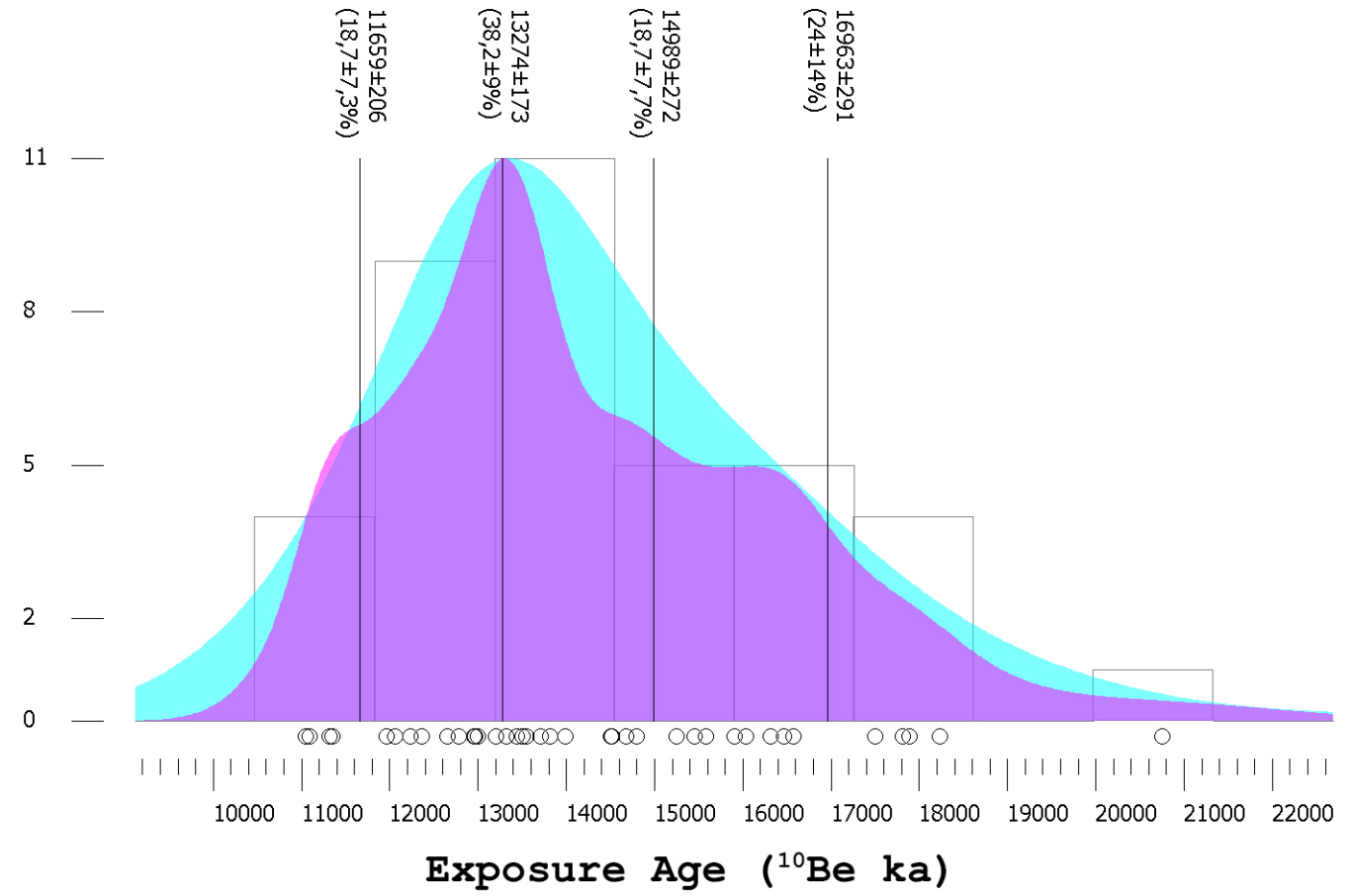

Fig. 4. Timing of rock glacier stabilization in the Western Tatra Mts. The probability density plot (purple shading) and Kernel Density Estimation (in cyan) of ^{10}Be exposure ages (n=39) obtained in this study and reported for rock glaciers in the Roháčska and Salatínska valleys by Engel et al. (2017). Vertical lines indicate mean ages with proportions for the modelled peaks and open circles show individual exposure ages (Vermeesch, 2012).

The timing of the rock glacier activity in the Western Tatra Mts. between ~18 and 11 ka (Fig. 4) is consistent with the major period of development of these landforms in other European mountain ranges. In accordance with local glaciation chronologies, the rock glacier stabilization in the Western Tatra Mts. (16.5 to 11 ka) took place around the same time as in the mountain ranges on the Iberian Peninsula (15.7 to 11.5 ka) but earlier than in the Alps (12.4 to 9.6 ka). The main phase of rock glacier stabilization overlaps with the GS-1 period, similarly as in the High Tatra Mts. (Zasadni et al., 2020), Alps (Moran et al., 2016; Charton et al., 2021), or Sierra Nevada (Palacios et al., 2016). The stabilization of rock glaciers in the mainland Europe terminated during the onset of the Holocene in the Tatra Mts. (Zasadni et al., 2020) and Alps (Ivy-Ochs and Schaller, 2009; Charton et al., 2021), while lasted until the mid-Holocene period in the Pyrenes (Andrés et al., 2018), Sierra Nevada (Palacios et al., 2016) and Tröllaskagi Peninsula, Iceland (Palacios et al., 2021).

5.2 Paleoclimatic and paleopermafrost implications

A minimum temperature declines relative to the present MAAT derived for the three oldest rock glaciers from the GS-2.1 is −3.9 °C and their fronts at ~1480 m asl are ~840 m lower compared to the present lower limit of discontinuous permafrost. These changes are close to the MAAT and elevation decrease of −3.7 to −3 °C and ~630−770 m, respectively, reported for the GS-2.1 rock glaciers in the High Tatra Mts. (Zasadni et al., 2020). On the other hand, these MAAT declines are much smaller than −10 to −9 °C derived for the GS-2.1 based on glacier modelling in the High Tatra Mts. (Makos et al., 2013, 2018). Similarly, the relevance of the GS-2.1 rock glaciers for the lower limit of discontinuous permafrost is also unclear because it is inconsistent with other local and regional paleopermafrost features (Fig. 5). Cryogenic-carbonate deposits found in caves in the High and Low Tatra Mts. indicate the presence of permafrost at ~670 m asl between ~17.1 ± 0.1 ka and ~15.2 ± 0.6 ka (Žák et al., 2012; Orvošová et al., 2014). Besides that, there is extensive evidence for at least discontinuous permafrost in the nearby Central European lowlands <~250 m asl as far south as 48°N between 18.1 ± 0.4 ka and 14.8 ± 0.1 ka based on the occurrence of relict frost wedges (Kovács et al., 2007; Fiedorczuk et al., 2007; Fábián et al., 2014; Ewertowski et al., 2017) and pingo scars (Hošek et al., 2020). This implies that permafrost was ubiquitous in the GS-2.1 and not limited to mountain areas. Considering the elevation of the lowermost GS-2.1 permafrost features in the Tatra Mts. and the nearby Central European lowlands of ~670 and ~60 m asl, respectively (Fig. 5), the MAAT decline in the GS-2.1 attains −7.7 °C and −10.5 °C, respectively. This is much closer to the MAAT decline reported by Makos et al. (2013, 2018) for the High Tatra Mts., as well as to the temperature decline of <−11 °C indicated by the lowland permafrost features (*sensu* Huijzer and Isarin, 1997; Huijzer and Vandenberghe, 1998). The plausibility of the larger MAAT decline also reflects the maximum elevation of the GS-2.1 rock glaciers (~rock glacier initiation altitude) of ~1610 m asl that fits the paleo-equilibrium line altitude at 1600–1700 m asl modelled in the High Tatra Mts. (Makos et al., 2013, 2018), as these two elevation indices are generally assumed to closely correspond (Humlum, 1998).

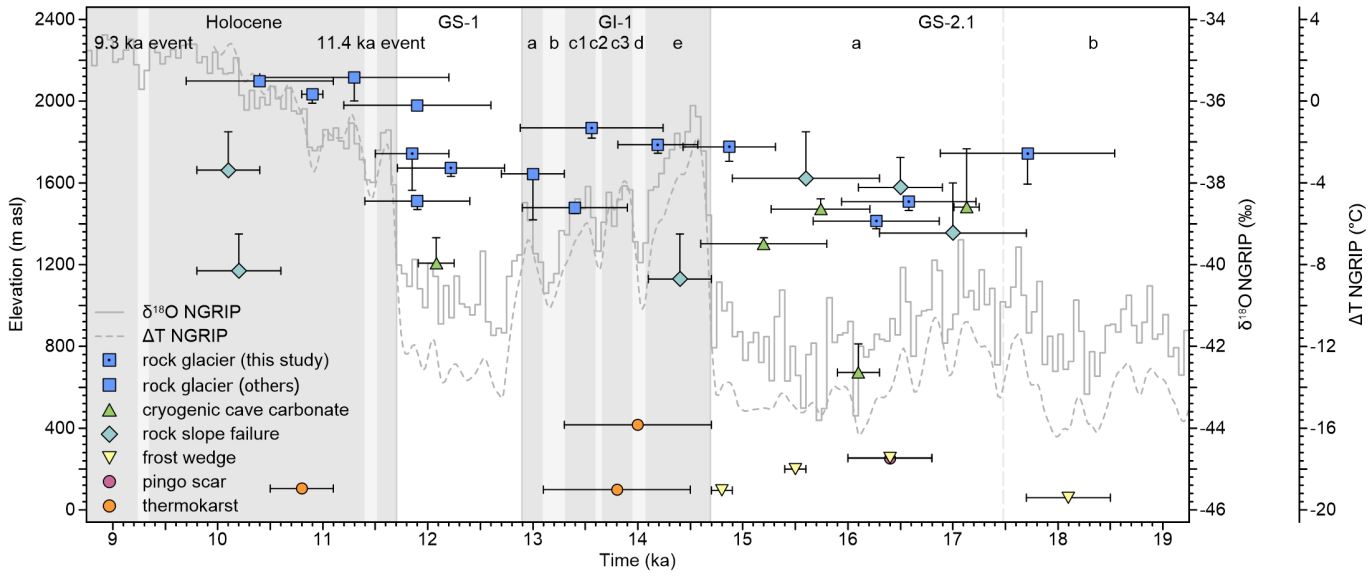

Fig. 5. Timing of rock glaciers and other paleopermafrost features around the Tatra Mts. Exposure ages for rock glaciers after Engel et al. (2017), Zasadni et al. (2020), and this study. Cryogenic cave carbonates (Žák et al., 2012; Orvošová et al., 2014), rock slope failures (Pánek et al., 2016), frost wedges (Kovács et al., 2007; Fiedorczuk et al., 2007; Fábián et al., 2014; Ewertowski et al., 2017), pingo scar (Hošek et al., 2020), and thermokarst features (Błaszkiewicz, 2011; Błaszkiewicz et al., 2015; Hošek et al., 2019)

constrain the timing of permafrost conditions or permafrost degradation. The arithmetic means and standard errors for individual locations are reported. Vertical bars show the elevation of rock glacier fronts, entrance of caves, and the lowest detachment zone for rock slope failures. The temperature offset (grey dashed line) relative to the present (Kindler et al., 2014), $\delta^{18}O$ data (grey solid line), and INTIMATE event stratigraphy (Rasmussen et al., 2014) are derived from the NGRIP ice core on the GICC05modelext time scale.

The three rock glaciers attributed to the GI-1 indicate a minimum MAAT decline of −2.5 °C and their fronts at ~1760 m asl suggest a decrease of the lower limit of discontinuous permafrost by ~560 m relative to the present. Engel et al. (2017) dated other two GI-1 rock glaciers in the study area at ~1440 m, which correspond to a MAAT decline of −4.1 °C and a decrease of the lower limit of discontinuous permafrost by ~880 m. These values seem reasonable because no other paleopermafrost features are present at lower elevations (Fig. 5) and there was a rapid climate warming at the onset of the GI-1 (Kindler et al., 2014), which prompted the thermokarst development in the nearby Central European lowlands between ~14.0 ± 0.7 cal. ka and ~13.8 ± 0.7 cal. ka (Błaszkiewicz, 2011; Błaszkiewicz et al., 2015; Hošek et al., 2019). Permafrost degradation may also have triggered a rock slope failure that initiated >1350 m asl at 14.4 ± 0.3 ka in the Western Tatra Mts. (Pánek et al., 2016). As rock glaciers tend to move faster with higher permafrost temperatures (Kääb et al., 2007), the warmer climate of the GI-1 may have enhanced the rock glaciers activity (Fig. 4), which could have been further promoted by a possible higher debris supply from collapsing slopes.

The two GS-1 rock glaciers suggest a MAAT decline of −3.4 °C and their fronts at ~1600 m asl correspond to a decrease of the lower limit of discontinuous permafrost by ~720 m. These indices differ from the values of −1.6 °C, ~2030 m asl, and ~335 m, respectively, reported by Zasadni et al. (2020) for rock glaciers in the High Tatra Mts. Nevertheless, there is another GS-1 rock glacier in the study area at ~1470 m asl (Engel et al., 2017) and a cryogenic-carbonate deposit in the Low Tatra Mts. further suggests that permafrost descended to at least ~1210 m asl 12.1 ± 0.2 ka (Fig. 5) (Orvošová et al., 2014), which implies a MAAT decline of at least −5.2 °C. This is plausible because the maximum elevation of the GS-1 rock glaciers of ~1830 m asl is just below the paleo-equilibrium line altitude at 1900 m asl modelled for the MAAT decline of −7 to −6 °C in the High Tatra Mts. (Makos et al., 2013, 2018). At the same time, it is consistent with the assumptions that only seasonally frozen ground existed in the nearby Central European lowlands south of 50°N in the GS-1 (Isarin, 1997), and isolated islands of permafrost occurred only in high mountain areas. The aforementioned discrepancies between the lower limit of the rock glaciers and other paleopermafrost features (Fig. 5) may result from topographic constraints, limited debris supply, unfavourable climatic conditions and/or insufficient time for development of the rock glaciers (Barsch, 1996; Kääb, 2013). Whatever the reason, the rock glaciers in the Western Tatra Mts. seem to underestimate past permafrost extents and temperature declines and should be used cautiously as paleoenvironmental proxies.

Since the beginning of the Holocene, climate warmed and permafrost degraded, which resulted in the final stabilization of the youngest rock glaciers at 1564–1632 m asl around 11.3 ± 0.4 ka. The increasing ground temperatures conditioned slope instability initiating rock slope failures >1850 m asl in the Western Tatra Mts. 10.2 ± 0.4 ka and 10.1 ± 0.3 ka (Pánek et al., 2016). The timing of the rapid

permafrost degradation is consistent with the peak of the thermokarst activity in northern Poland at ~10.8 ± 0.3 cal. ka (Błaszkiewicz, 2011; Błaszkiewicz et al., 2015).

6 Conclusions

The dataset of ^{10}Be exposure ages obtained for rock glaciers in the Western Tatra Mts., Western Carpathians, documents their activity between ~18 and 11 ka. This activity is attributed to three main phases: (1) 17.7 ± 0.8 to 16.3 ± 0.6 ka, (2) 14.9 ± 0.4 to 13.6 ± 0.7 ka, and (3) 12.2 ± 0.5 to 11.9 ± 0.4 ka. The oldest dated rock glaciers with front elevation of 1376–1594 m asl started to form during the Greenland Stadial 2.1 following the retreat of glaciers from their LGM positions. The middle phase of activity reflects warm conditions during the Greenland Interstadial 1 and the youngest landforms coincide with the Greenland Stadial 1 (~Younger Dryas). The final stabilization of the youngest rock glaciers with fronts located at an elevation of 1564–1632 m asl probably lasted until the beginning of the Holocene as indicate exposure ages of 11.3 ± 0.4 and 11.1 ± 0.6 ka obtained for boulders at the northern foot of the main mountain ridge.

The initiation altitude of ~1610 and 1830 m determined for the rock glaciers from the Greenland Stadials 2.1 and 1, respectively, is consistent with estimates of the paleo-equilibrium line altitude reported for these periods. However, the lower limit of the rock glaciers is well above other regional paleopermafrost features from the same periods. This suggests that elevation indices derived for the rock glaciers in the Western Tatra Mts. underestimate past permafrost extents and temperature declines raising questions about their validity for paleoenvironmental reconstructions.

Funding

This research was supported by the Charles University Grant Agency (project no. 1528119) and the Czech Science Foundation (project 21-23196S).

ASTER AMS national facility (CEREGE, Aix-en-Provence, France) is supported by the INSU/CNRS, and IRD.

Declaration of competing interest

The authors declare that they have no known competing financial interests or personal relationships that could have appeared to influence the work reported in this paper.

Acknowledgements

The Tatra National Park Administration is thanked for providing permission to work in the protected area.

References

Andrés, N., Gómez-Ortiz, A., Fernández-Fernández, J. M., Tanarro, L. M., Salvador-Franch, F., Oliva, M., Palacios, D., 2018. Timing of deglaciation and rock glacier origin in the southeastern Pyrenees: a review and new data. Boreas, 47(4), 1050-1071. https://doi.org/10.1111/bor.12324

Arnold, M., Merchel, S., Bourlès, D.L., Braucher, R., Benedetti, L., Finkel, R.C., Aumaître, G., Gottdang, A., Klein, M., 2010. The French accelerator mass spectrometry facility ASTER: improved performance and developments. Nucl. Instrum. Methods Phys. Res., Sect. B 268, 1954-1959. https://10.1016/j.nimb.2010.02.107

Balco, G., Stone, J.O., Lifton, N.A., Dunai, T.J., 2008. A complete and easily accessible means of calculation surface exposure ages or erosion rates from 10Be and 26Al measurements. Quaternary Geochronology 3, 174-195. https://doi.org/10.1016/j.quageo.2007.12.001

Ballantyne, C. K., Schnabel, C., Xu, S., 2009. Exposure dating and reinterpretation of coarse debris accumulations ('rock glaciers') in the Cairngorm Mountains, Scotland. Journal of Quaternary Science: Published for the Quaternary Research Association, 24(1), 19-31. https://doi.org/10.1002/jqs.1189

Ballantyne, C. K., 2018. Periglacial Geomorphology. Wiley-Blackwell, Hoboken.

Barsch, D., 1996. Rockglaciers: indicators for the present and former geoecology in high mountain environments (Vol. 16). Berlin Heidelberg. Springer Science & Business Media.

Baumgart-Kotarba M. and Kráľ, J., 2002. Young tectonic uplift of the Tatra Mts (Fission track data and geomorphological arguments). Proceedings of XVII. Congress of Carpathian-Balkan Geological Association. Geol. Carpathica, Spec. Issue, 53.

Błaszkiewicz, M., 2011. Timing of the final disappearance of permafrost in the central European Lowland, as reconstructed from the evolution of lakes in N Poland. Geol. Quart. 55, 361–374.

Błaszkiewicz, M., Piotrowski, J. A., Brauer, A., Gierszewski, P., Kordowski, J., Kramkowski, M., Lamparski, P., Lorenz, S., Noryśkiewicz, A. M., Ott, F., Słowiński, M., Tyszkowski, S., 2015. Climatic and morphological controls on diachronous postglacial lake and river valley evolution in the area of Last Glaciation, northern Poland. Quat. Sci. Rev. 109, 13–27. https://doi.org/10.1016/j.quascirev.2014.11.023.

Blomdin, R., Stroeven, A.P., Harbor, J.M., Lifton, N.A., Heyman, J., Gribenski, N., Petrakov, D.A., Caffee, M.W., Ivanov, M.N., Hättestrand, C., Rogozhina, I., Usubaliev, R., 2016. Evaluating the timing of former glacier expansions in the Tian Shan: A key step towards robust spatial correlations. Quat. Sci. Rev. 153, 78-96. https://10.1016/j.quascirev.2016.07.029

Böhlert, R., Compeer, M., Egli, M., Brandová, D., Maisch, M., Kubik, P. W., Haeberli, W., 2011. A combination of relative-numerical dating methods indicates two high Alpine rock glacier activity phases after the glacier advance of the Younger Dryas. Open Geography Journal, (4), 115-130. https://doi.org/10.2174/1874923201104010115

Borchers, B., Marrero, S., Balco, G., Caffee, M., Goehring, B., Lifton, N., Nishiizumi, K.,Phillips, F., Schaefer, J., Stone, J., 2016. Geological calibration of spallation production rates in the CRONUS-Earth project. Quat. Geochronol. 31, 188 -198. https://doi:10.1016/j.quageo.2015.01.009

Braucher, R., Merchel, S., Borgomano, J., Bourlès, D.L., 2011. Production of cosmogenic radionuclides at great depth: a multi element approach. Earth Planet Sci Lett. 309(1–2), 1–9. 10.1016/j.epsl.2011.06.036

Braucher R., Guillou V., Bourlès D.L., Arnold M., Aumaître G., Keddadouche K., Nottoli E., 2015. Preparation of ASTER in-house10Be/9Be standard solutions. Nuclear Instruments and Methods in Physics Research B 361, 335-340. https://doi.org/10.1016/j.nimb.2015.06.012

Charton, J., Verfaillie, D., Jomelli, V., Francou, B., ASTER Team., 2021. Early Holocene rock glacier stabilisation at col du Lautaret (French Alps): Palaeoclimatic implications. Geomorphology, 394, 107962. https://doi.org/10.1016/j.geomorph.2021.107962

Chmeleff, J., von Blanckenburg, F., Kossert, K., Jakob, D., 2010. Determination of the 10Be half-life by multicollector ICP-MS and liquid scintillation counting. Nucl. Instr. Meth. B 263(2), 192-199. https://doi.org/10.1016/j.nimb.2009.09.012

Colucci, R. R., Boccali, C., Žebre, M., & Guglielmin, M., 2016. Rock glaciers, protalus ramparts and pronival ramparts in the south-eastern Alps. Geomorphology, 269, 112-121. https://doi.org/10.1016/j.geomorph.2016.06.039

Denn, A.R., Bierman, P.R., Zimmerman, S.R.H., Caffee, M.W., Corbett, L.B., Kirby, E., 2018. Cosmogenic nuclides indicate that boulder fields are dynamic, ancient, multigenerational features. GSA Today 28, 4–10. https://doi.org/10.1130/GSATG340A.1

Dlabáčková, T., Engel, Z., 2022. Rainfall Thresholds of the 2014 Smutna Valley Debris Flow in Western Tatra Mountains, Carpathians, Slovakia. AUC Geographica, 57(1), 3-15. https://doi.org/10.14712/23361980.2022.1

Dobiński, W., 2005. Permafrost of the Carpathian and Balkan Mountains, eastern and southeastern Europe. Permafrost and Periglacial Processes, 16(4), 395-398. https://doi.org/10.1002/ppp.524

Dunai, T.J., 2010. Cosmogenic Nuclides – Principles, concepts and applications in the Earth Surface Sciences. Cambridge University Press, New York.

Dunne, J., Elmore, D., Muzikar, P., 1999. Scaling factors for the rates of production of cosmogenic nuclides for geometric shielding and attenuation at depth on sloped surfaces. Geomorphology 27(1-2), 3-11. https://doi:10.1016/S0169-555X(98)00086-5

Engel, Z., Mentlík, P., Braucher, R., Křížek, M., Pluháčková, ASTER Team, 2017. 10Be exposure age chronology of the last glaciation of the Rohačska Valley in the Western Tatra Mountains, central Europe. Geomorphology, 293, 130-142. https://doi.org/10.1016/j.geomorph.2017.05.012

Ewertowski, M.W., Kijowski, A., Szuman, I., Tomczyk, A.M., Kasprzak, L., 2017. Low-altitude remote sensing and GIS-based analysis of cropmarks: classification of past thermal-contraction-crack polygons in

central western Poland. Geomorphology 293, 418–432. https://doi.org/10.1016/j.geomorph.2016.07.022.

Fábián, S.Á., Kovács, J., Varga, G., Sipos, G., Horváth, Z., Thamó-Bozsó, E., Tóth, G., 2014. Distribution of relict permafrost features in the Pannonian Basin, Hungary. Boreas 43, 722–732. https://doi.org/10.1111/bor.12046.

Fernández-Fernández, J. M., Palacios, D., Andrés, N., Schimmelpfennig, I., Tanarro, L. M., Brynjólfsson, López-Acevedo, F. J., Sæmundsson, Þ., ASTER Team., 2020. Constraints on the timing of debris-covered and rock glaciers: an exploratory case study in the Hólar area, northern Iceland. Geomorphology, 361, 107196. https://doi.org/10.1016/j.geomorph.2020.107196

Fiedorczuk, J., Bratlund, B., Kolstrup, E., Schild, R., 2007. Late Magdalenian feminine flint plaquettes from Poland. Antiquity 81, 97–105. https://doi.org/10.1017/S0003598X00094862

Frauenfelder, R., Haeberli, W., Hoelzle, M., Maisch, M., 2001. Using relict rockglaciers in GIS-based modelling to reconstruct Younger Dryas permafrost distribution patterns in the Err-Julier area, Swiss Alp. Norsk Geografisk Tidsskrift - Norwegian Journal of Geography, 55:4, 195-202, 10.1080/00291950152746522

Frauenfelder, R., Laustela, M., Kääb, A., 2005. Relative age dating of Alpine rockglacier surfaces. Zeitschrift für Geomorphologie, 49(2), 145-166.

French, H. M., 2017. The periglacial environment. 4th ed. Chichester: John Wiley. ISBN: 978-1-119-13278-3

Gądek, B., 2014. Climatic sensitivity of the non-glaciated mountains cryosphere (Tatra Mts., Poland and Slovakia). Global and Planetary Change, 121, 1-8. https://doi.org/10.1016/j.gloplacha.2014.07.001

García-Ruiz, J. M., Palacios, D., Fernández-Fernández, J. M., Andrés, N., Arnáez, J., Gómez-Villar, A., Santos-González, J., Álvarez-Martínez, J., Lana-Renault, N., Léanni, L., ASTER Team, 2020. Glacial stages in the Peña Negra valley, Iberian Range, northern Iberian Peninsula: Assessing the importance of the glacial record in small cirques in a marginal mountain area. Geomorphology, 362, 107195. https://doi.org/10.1016/j.geomorph.2020.107195

Geodetic and Cartographic Institute Bratislava, National Forest Centre, 2021. Orthophotomosaic of the Slovak Republic.

Gosse, J.C., Phillips, F.M., 2001. Terrestrial in situ cosmogenic nuclides: theory and application. Quaternary Sci Rev. 20, 1475–560. https://doi:10.1016/S0277-3791(00)00171-2

Haeberli, W., King, L., Flotron, A., 1979. Surface movement and lichen cover studies at the active rock glacier near the Grubengletscher, Wallis, Swiss Alps. Arctic and Alpine Research 11(4). 421–441.

Haeberli, W., 1985. Creep of mountain permafrost: Internal structure and flow of alpine rock glaciers. Mitteilungen der Versuchsanstalt für Wasserbau, Hydrologie und Glaziologie, 77, 1–142.

Hamilton, S. J. and Whalley, W. B., 1995. Preliminary results from the lichenometric study of the Nautardálur rock glacier, Tröllaskagi, northern Iceland. Geomorphology, 12(2), 123-132. https://doi.org/10.1016/0169-555X(94)00083-4

Hippolyte, J. C., Bourlès, D., Braucher, R., Carcaillet, J., Léanni, I., Arnold, M., Aumaitre, G., 2009. Cosmogenic 10Be dating of a sackung and its faulted rock glaciers, in the Alps of Savoy (France). Geomorphology, 108(3-4), 312-320. https://doi.org/10.1016/j.geomorph.2022.108112

Hošek, J., Prach, J., Křížek, M., Šída, P., Moska, P., Pokorný, P., 2019. Buried Late Weichselian thermokarst landscape discovered in the Czech Republic, central Europe. Boreas 48, 988–1005. https://doi.org/10.1111/bor.12404.

Hošek, J., Radoměřský, T., Křížek, M., 2020. Pozdně glaciální termokrasové jevy na severním okraji víděňské pánve (Late Glacial thermokarst phenomena on the northern margin of the Vienna Basin (Czech Republic) (in Czech). Geosci. Res. Rep. 53, 65−72. https://doi.org/10.3140/zpravy.geol.2020.42.

Huijzer, A.S., Isarin, R.F.B., 1997. The reconstruction of past climates using multi-proxy evidence: An example of the weichselian pleniglacial in northwest and central Europe. Quat. Sci. Rev. 16, 513−533. https://doi.org/10.1016/S0277-3791(96)00080-7.

Huijzer, B., Vandenberghe, J., 1998. Climatic reconstruction of the Weichselian Pleniglacial in northwestern and central Europe. J. Quat. Sci. 13, 391–417. https://doi.org/10.1002/(SICI)1099-1417(1998090)13:5<391::AID-JQS397>3.0.CO;2-6.

Humlum, O., 1998. The climatic significance of rock glaciers. Permafr. Periglac. Process. 9, 375–395. https://doi.org/10.1002/(SICI)1099-1530(199810/12)9:4%3C375::AID-PPP301%3E3.0.CO;2-0.

Isarin, R.F.B., 1997. Permafrost Distribution and Temperatures in Europe During the Younger Dryas. Permafr. Periglac. Process. 8, 313–333. https://doi.org/10.1002/(SICI)1099-1530(199709)8:3%3C313::AID-PPP255%3E3.0.CO;2-E.

Ivy-Ochs, S., Kerschner, H., Reuther, A., Maisch, M., Sailer, R., Schaefer, J., Kubik, P. V., Synal, H.-A., Schlüchter, C., 2006. The timing of glacier advances in the northern European Alps based on surface exposure dating with cosmogenic ^{10}Be, ^{26}Al, ^{36}Cl, and ^{21}Ne. Special Papers-Geological Society of America, 415, 43.

Ivy-Ochs, S., Kerschner, H., Maisch, M., Christl, M., Kubik, P. W., Schlüchter, C., 2009: Latest Pleistocene and Holocene glacier variations in the European Alps. Quaternary Science Reviews, 28(21-22), 2137-2149. https://doi.org/10.1016/j.quascirev.2009.03.009

Ivy-Ochs, S., Schaller, M., 2009. Examining processes and rates of landscape change with cosmogenic radionuclides. In: Froehlich, K. (Ed.), Radioactivity in the Environment. Elsevier, Amsterdam, pp. 231–294.

Jacko, S., Labant, S., Bátorová, K., Farkašovský, R., Ščerbáková, B., 2021. Structural contraints of neotectonic activity in the eastern part of the Western Carpathians orogenic wedge. Quaternary International, 585, 27-43. https://doi.org/10.1016/j.quaint.2020.10.072

Jurewicz, E., 2007. Multistage evolution of the granitoid core in Tatra Mountains. Granitoids in Poland. Warsaw University, Warsaw, 307-317.

Kääb, A., Gudmundsson, G. H., Hoelzle, M., 1998. Surface deformation of creeping mountain permafrost. Photogrammetric investigations on Murtèl rock glacier, Swiss Alps. In Proceedings of the Seventh International Conference on Permafrost, 531-537.

Kääb, A., Frauenfelder, R., Roer, I., 2007. On the response of rockglacier creep to surface temperature increase. Glob. Planet. Change 56, 172–187. https://doi.org/10.1016/j.gloplacha.2006.07.005.

Kääb, A., 2013. Rock glaciers and protalus forms. In S. A. Elias and C. J. Mock (Eds.), Encyclopedia of Quaternary science (2nd ed.), Amsterdam: Elsevier, 535–541.

Kellerer-Pirklbauer, A., 2008a. The Schmidt-hammer as a relative age dating tool for rock glacier surfaces: examples from Northern and Central Europe. In Proceedings of the Ninth International Conference on Permafrost (NICOP), University of Alaska, Fairbanks, 913-918.

Kellerer-Pirklbauer, A., Wangensteen, B., Farbrot, H., Etzelmüller, B., 2008b. Relative surface age-dating of rock glacier systems near Hólar in Hjaltadalur, Northern Iceland. Journal of Quaternary Science: Published for the Quaternary Research Association, 23(2), 137-151. https://doi.org/10.1002/jqs.1117

Kellerer-Pirklbauer, A., Lieb, G. K., & Kleinferchner, H., 2012. A new rock glacier inventory of the Eastern European Alps. Austrian Journal of Earth Sciences, 105(2).

Kindler, P., Guillevic, M., Baumgartner, M., Schwander, J., Landais, A., Leuenberger, M., 2014. Temperature reconstruction from 10 to 120 kyr b2k from the NGRIP ice core, Clim. Past 10, 887–902. https://doi.org/10.5194/cp-10-887-2014.

Kłapyta, P., 2009. Glacial and periglacial relief on the southern slopes of the Western Tatra Mts. (Slovakia) – The results of the first detailed geomorphological mapping of the Žiarska, Jamnicka, Račkova and Bystra Valleys. Landform Analysis, 10, 50–57.

Kłapyta, P., 2011. Relative surface dating of rock glacier systems in the Žiarska Valley, the Western Tatra Mountains, Slovakia. Studia Geomorphologica Carpatho-Balcanica, 45, 89–106.

Kłapyta, P., 2013. Application of Schmidt hammer relative age dating to Late Pleistocene moraines and rock glaciers in the Western Tatra Mountains, Slovakia. Catena, 111, 104–121. 10.1016/j.catena.2013.07.004

Kłapyta, P., 2015. Relief of selected parts of the Western Tatra Mountains. In: K. Dabrowska, M. Guzik (Eds.), Atlas of the Tatra Mountains: Abiotic Nature. TPN, Zakopane.

Kłapyta, P., Zasadni, J., Pociask-Karteczka, J., Gajda, A., Franczak, P., 2016. Late Glacial and Holocene paleoenvironmental records in the Tatra Mountains, East-Central Europe, based on lake, peat bog and colluvial sedimentary data: A summary review. Quaternary International, 415, 126-144. https://doi.org/10.1016/j.quaint.2015.10.049

Kočický, D., 1996. Charakteristiky snehovej pokrývky v oblasti Tatier v období 1960/61-1989/90. Unpublished diploma thesis. Comenius University in Bratislava. In Slovak

Korschinek, G., Bergmaier, A., Faestermann, T., Gerstmann, U.C., Knie, K., Rugel, G., Wallner, A., 2010. A new value for the half-life of 10Be by heavy-ion elastic recoil detection and liquid scintillation counting. Nucl. Instr. Meth. B 268(2), 187-191. https://doi:10.1016/j.nimb.2009.09.020

Kotarba, A. 1992: Natural environment and landform dynamics of the Tatra Mountains. Mountain Research and Development, 105-129. https://doi.org/10.2307/3673786

Kovács, J., Fábián, S.Á., Schweitzer, F., Varga, G. 2007. A relict sand-wedge polygon site in north-central Hungary. Permafr. Periglac. Process. 18, 379–384. https://doi.org/10.1002/ppp.600.

Krainer, K., Bressan, D., Dietre, B., Haas, J. N., Hajdas, I., Lang, K., Mair, V., Nickus, U., Reidl, D., Thies, H., Tonidandel, D., 2015. A 10,300-year-old permafrost core from the active rock glacier Lazaun, southern Ötztal Alps (South Tyrol, northern Italy). Quaternary Research, 83(2), 324-335. https://doi.org/10.1016/j.yqres.2014.12.005

Králiková, S., Vojtko, R., Sliva, U., Minár, J., Fuegenschuh, B., Kovac, M., Hok, J., 2014. Cretaceous-Quaternary tectonic evolution of the Tatra Mts (Western Carpathians): constraints from structural, sedimentary, geomorphological, and fission track data. Geologica Carpathica, 65(4), 307. 10.2478/geoca-2014-0021

Laustela, M., Egli, M., Frauenfelder, R., Kääb, A., Maisch, M., Haeberli, W., 2003. Weathering rind measurements and relative age dating of rockglacier surfaces in crystalline regions of the Eastern Swiss Alps. In Proceedings of the 8th International Conference on Permafrost, Zürich, Switzerland, 627-632.

Lindner, L., Dzierżek, J., Marciniak, B., & Nitychoruk, J., 2003. Outline of Quaternary glaciations in the Tatra Mts.: their development, age and limits. Geological Quarterly, 47(3), 269-280.

Linge, H., Nesje, A., Matthews, J. A., Fabel, D., Xu, S., 2020. Evidence for rapid paraglacial formation of rock glaciers in southern Norway from 10Be surface-exposure dating. Quaternary Research, 55-70. https://doi.org/10.1017/qua.2020.10

Makos, M., Nitychoruk, J., Zreda, M., 2013. Deglaciation chronology and paleoclimate of the Pięciu Stawów Polskich/Roztoki Valley, high Tatra Mountains, Western Carpathians, since the Last Glacial Maximum, inferred from 36Cl exposure dating and glacier–climate modelling. Quat. Int. 293, 63–78. https://doi.org/10.1016/j.quaint.2012.01.016.

Makos, M., Rinterknecht, V., Braucher, R., Żarnowski, M., Aster Team, 2016. Glacial chronology and palaeoclimate in the Bystra catchment, western Tatra Mountains (Poland) during the late Pleistocene. Quat. Sci. Rev. 134, 74–91. http://dx.doi.org/10.1016/j.quascirev.2016.01.004.

Matthews, J. A., Nesje, A., Linge, H., 2013. Relict talus-foot rock glaciers at Øyberget, upper Ottadalen, southern Norway: Schmidt hammer exposure ages and palaeoenvironmental implications. Permafrost and Periglacial Processes, 24(4), 336-346. https://doi.org/10.1002/ppp.1794

Matthews, J. A., Winkler, S., 2022. Schmidt-hammer exposure-age dating: a review of principles and practice. Earth-Science Reviews, 104038. https://doi.org/10.1016/j.earscirev.2022.104038.

Moran, A. P., Ochs, S. I., Vockenhuber, C., Kerschner, H., 2016. Rock glacier development in the Northern Calcareous Alps at the Pleistocene-Holocene boundary. Geomorphology, 273, 178-188. https://doi.org/10.1016/j.geomorph.2016.08.017

Niedzwiedz, T., 1992. Climate of the Tatra Mountains. Mountain Research and Development, 131-146. https://doi.org/10.2307/3673787

Niedźwiedź, T., Łupikasza, E., Pińskwar, I., Kundzewicz, Z. W., Stoffel, M., Małarzewski, Ł., 2015: Variability of high rainfalls and related synoptic situations causing heavy floods at the northern foothills of the Tatra Mountains. Theoretical and Applied Climatology, 119(1), 273-284. https://doi.org/10.1007/s00704-014-1108-0.

Nemčok, A., Mahr, T., 1974. Kamenné ľadovce v Tatrách (Fossil rock glaciers in Tatras). Geografický časopis, 26, 359–373.

Nemčok, J., Bezák, V., Biely, A., Gorek, A., Gross, P., Halouzka, R., … Zelman, J., 1994. Geologická mapa Tatier 1 : 50 000 [Geological map of the Tatra Mts. 1 : 50 000]. Bratislava: State Geological Institute of Dionýz Štúr.

Nicholas, J.W., Butler, D.R., 1996. Application of relative-age dating techniques on rock glaciers of the La Sal Mountains, Utah: an interpretation of Holocene paleoclimates. Geografiska Annaler 78, 1–18.

Obidowicz, A., 1996. A Late glacial-Holocene history of the formation of vegetation belts in the Tatra Mts. Acta Paleobotanica 36 (2), 159−206.

Orvošová, M., Deininger, M., Milovský, R, 2014. Permafrost occurrence during the Last Permafrost Maximum in the Western Carpathian Mountains of Slovakia as inferred from cryogenic cave carbonate. Boreas 43, 750−758. https://doi.org/10.1111/bor.12042.

Palacios, D., Andrés, N., López-Moreno, J., García-Ruiz, J. M., 2015. Late Pleistocene deglaciation in the upper Gállego valley, Central Pyrenees. Quaternary Research, 83, 397-414. https://doi.org/10.1016/j.yqres.2015.01.010

Palacios, D., Gómez-Ortiz, A., Andrés, N., Salvador, F., Oliva, M., 2016. Timing and new geomorphologic evidence of the last deglaciation stages in Sierra Nevada (southern Spain). Quaternary Science Reviews, 150, 110-129. https://doi.org/10.1016/j.quascirev.2016.08.0127

Palacios, D., Rodríguez-Mena, M., Fernández-Fernández, J. M., Schimmelpfennig, I., Tanarro, L. M., Zamorano, J. J., Andrés, N., Úbeda, J., Sæmundsson, Þ., Brynjólfsson, S., Oliva, M., ASTER Team., 2021. Reversible glacial-periglacial transition in response to climate changes and paraglacial dynamics: a case study from Héðinsdalsjökull (northern Iceland). Geomorphology, 388, 107787. https://doi.org/10.1016/j.geomorph.2021.107787

Pánek, T., Engel, Z., Mentlík, P., Braucher, R., Břežný, M., Škarpich, V., Zondervan, A., 2016. Cosmogenic age constraints on post-LGM catastrophic rock slope failures in the Tatra Mountains (Western Carpathians). Catena 138, 52–67. https://doi.org/10.1016/j.catena.2015.11.005.

Pánek, T., Minár, J., Vitovič, L., Břežný, M., 2020. Post-LGM faulting in Central Europe: LiDAR detection of the >50 km-long Sub-Tatra fault, Western Carpathians. Geomorphology, 364, 107248. https://doi.org/10.1016/j.geomorph.2020.107248

Rasmussen, S. O., Bigler, M., Blockley, S. P., Blunier, T., Buchardt, S. L., Clausen, H. B., Cvijanovic, I., Dahl-Jensen, D., Johnsen, S. J., Fischer, H., Gkinis, V., Guillevic, M., Hoek, W. Z., Lowe, J. J., Pedro, J. B., Popp, T., Seierstad, I. K., Steffensen, J. P., Svensson, A. M., Vallelonga, P., Vinther, B. M., Walker, M. J. C., Wheatley, J. J., Winstrup, M., 2014. A stratigraphic framework for abrupt climatic changes during the Last Glacial period based on three synchronized Greenland ice-core records: refining and extending the INTIMATE event stratigraphy. Quat. Sci. Rev. 106, 14–28. https://doi.org/10.1016/j.quascirev.2014.09.007.

Refsnider, K.A., Brugger, K.A., 2007. Rock glaciers in central Colorado as indicators of late- Holocene climate change: a lichenometric study using Rhizocarpon subgenus Rhizocarpon. Arctic, Antarctic and Alpine Research 39, 127–136.

RGIK, 2022. Towards standard guidelines for inventorying rock glaciers: practical concepts (version 2.0). IPA Action Group Rock glacier inventories and kinematics, 10 pp.

Rode, M. and Kellerer-Pirklbauer, A., 2012. Schmidt-hammer exposure-age dating (SHD) of rock glaciers in the Schöderkogel-Eisenhut area, Schladminger Tauern Range, Austria. The Holocene, 22(7), 761-771. https://doi.org/10.1177/0959683611430410

Rodríguez-Rodríguez, L., Jiménez-Sánchez, M., Domínguez-Cuesta, M. J., Rinterknecht, V., Pallas, R., and Bourles, D., 2016. Chronology of glaciations in the Cantabrian Mountains (NW Iberia) during the Last Glacial Cycle based on in situ-produced 10Be. Quaternary Science Reviews, 138, 31-48. https://doi.org/10.1016/j.quascirev.2016.02.027

Rodríguez-Rodríguez, L., Jiménez-Sánchez, M., Domínguez-Cuesta, M. J., Rinterknecht, V., Pallàs, R., AsterTeam, 2017. Timing of last deglaciation in the Cantabrian Mountains (Iberian Peninsula; North Atlantic Region) based on in situ-produced 10Be exposure dating. Quaternary Science Reviews, 171, 166-181. https://doi.org/10.1016/j.quascirev.2017.07.012

Santos-González, J., González-Gutiérrez, R. B., Redondo-Vega, J. M., Gómez-Villar, A., Jomelli, V., Fernández-Fernández, J. M., Andrés, N., García-Ruiz, J. M., Peña-Pérez, S. A., Melón-Nava, A., Oliva, M., Álvarez-Martínez, J., Charton, J., ASTER Team, Palacios, D., 2022. The origin and collapse of rock glaciers during the Bølling-Allerød interstadial: A new study case from the Cantabrian Mountains (Spain). Geomorphology, 401, 108112. https://doi.org/10.1016/j.geomorph.2022.108112

Scapozza, C., Lambiel, C., Reynard, E., Fallot, J. M., Antognini, M., Schoeneich, P., 2010. Radiocarbon dating of fossil wood remains buried by the Piancabella rock glacier, Blenio Valley (Ticino, Southern Swiss Alps): implications for rock glacier, treeline and climate history. Permafrost and Periglacial Processes, 21(1), 90-96. https://doi.org/10.1002/ppp.673

State Geological Institute of Dionýz Štúr, 2013. Geological map of Slovakia M 1:50 000. http://apl.geology.sk/gm50js/ (accessed 6 March 2021).

Steinemann, O., Reitner, J. M., Ivy-Ochs, S., Christl, M., Synal, H. A., 2020. Tracking rockglacier evolution in the Eastern Alps from the Lateglacial to the early Holocene. Quaternary Science Reviews, 241, 106424. https://doi.org/10.1016/j.quascirev.2020.106424

Stone, J.O., 2000. Air pressure and cosmogenic isotope production. J. Geophys. Res. 105 (B10), 23753–23759. http://dx.doi.org/10.1029/2000JB900181.

The Geodesy, Cartography and Cadastre Authority of the Slovak Republic, 2018. Airborne laser scanning and DEM 5.0. Site No. 26 (Tatra Mts.).

Ustrnul, Z., Walawender, E., Czekierda, D., Šťastný, P., Lapin, M., Mikulová, K., 2015. Precipitation and snow cover. In: K. Dabrowska, M. Guzik (Eds.), Atlas of the Tatra Mountains: Abiotic Nature. TPN, Zakopane.

Uxa, T., Mida, P., 2017. Rock glaciers in the western and high Tatra mountains, western Carpathians. Journal of Maps, 13(2), 844-857. https://doi.org/10.1080/17445647.2017.1378136

Vermeesch, P., 2012. On the visualisation of detrital age distributions. Chem. Geol. 312−313, 190−194. https://doi.org/10.1016/j.chemgeo.2012.04.021

Vasile, M., Vespremeanu-Stroe, A., Pascal, D., Braucher, R., Pleșoianu, A., Popescu, R., Etzelmüller, B., ASTER Team., 2022. Rock walls distribution and Holocene evolution in a mid-latitude mountain range (the Romanian Carpathians). Geomorphology, 413, 108351. https://doi.org/10.1016/j.geomorph.2022.108351

Vespremeanu-Stroe, A., Urdea, P., Popescu, R., Vasile, M., 2012. Rock glacier activity in the Retezat mountains, Southern Carpathians, Romania. Permafr. Periglac. Process, 23, 127–137. https://doi.org/10.1002/ppp.1736.

Vitovič, L., Minár, J., Pánek, T., 2021. Morphotectonic configuration of the Podtatranská Kotlina Basin and its relationship to the origin of the Western Carpathians. Geomorphology, 394, 107963. https://doi.org/10.1016/j.geomorph.2021.107963

Ward, G. K. and Wilson, S. R., 1978. Procedures for comparing and combining radiocarbon age determinations: a critique. Archaeometry, 20(1), 19-31.

Žák, K., Richter, D. K., Filippi, M., Živor, R., Deininger, M., Mangini, A., Scholz, D., 2012. Coarsely crystalline cryogenic cave carbonate – a new archive to estimate the Last Glacial minimum permafrost depth in Central Europe, Clim. Past. 8, 1821–1837. https://doi.org/10.5194/cp-8-1821-2012.

Zasadni, J., Kłapyta, P., 2009. An attempt to assess the modern and the Little Ice Age climatic snowline altitude in the Tatra Mountains. Landform Analysis, 10, 124-133.

Zasadni, J. and Kłapyta, P., 2016. From valley to marginal glaciation in alpine-type relief: Lateglacial glacier advances in the Pięć Stawów Polskich/Roztoka Valley, High Tatra Mountains, Poland. Geomorphology, 253, 406–424. https://10.1016/j.geomorph.2015.10.032

Zasadni, J., Kłapyta, P., Broś, E., Ivy-Ochs, S., Świąder, A., Christl, M., & Balážovičová, L., 2020. Latest Pleistocene glacier advances and post-Younger Dryas rock glacier stabilization in the Mt. Kriváň group, High Tatra Mountains, Slovakia. Geomorphology, 358, 107093. https://doi.org/10.1016/j.geomorph.2020.107093

Zasadni, J., Kłapyta, P., Makos, M., 2022. The evolution of glacial landforms in the Tatra Mountains during the Bølling-Allerød Interstadial. In: Palacios, D., Hughes, P. D., Garcia-Ruiz, J. M., de Andrés, N. (Eds.), European Glacial Landscapes: The Last Deglaciation. Elsevier. https://doi.org/10.1016/C2020-0-00404-4

Żmudzka, E., Nejedlík, P., Mikulová, K., 2015. Temperature, thermal indices. In: K. Dabrowska, M. Guzik (Eds.), Atlas of the Tatra Mountains: Abiotic Nature. TPN, Zakopane.

Table A.1. Location and site characteristics of the sampled boulders.

Rock glacier	Sample	Latitude (°N)	Longitude (°W)	Elevation (m asl)	Length/width /height (m)	Surface aspect/dip (°)	Topographic shielding factor	Snow cover depth/duration (cm/month)
Jamnícka -North	JAM-1	49.195247	19.757970	1779	5.5/1.4/1.7	105/9	0.97361	55/7
	JAM-2	49.195336	19.758028	1789	1.8/1.7/1.6	265/3	0.95823	49/6
	JAM-3	49.195574	19.757766	1791	2.1/2.0/1.8	75/4	0.95362	50/6
	JAM-4	49.195509	19.757790	1785	3.2/2.5/1.4	270/3	0.95040	50/6
	JAM-5	49.194880	19.756940	1793	2.7/0.9/1.9	horizontal	0.95306	50/6
Jamnícka -South	JAM-6	49.191861	19.763420	1659	3.1/2.4/2.8	horizontal	0.94499	39/6
	JAM-7	49.191783	19.763369	1680	1.6/1.5/1.3	135/12	0.94312	39/6
	JAM-8	49.191676	19.763368	1680	3.4/2.6/1.9	horizontal	0.94325	39/6
	JAM-9	49.192111	19.763369	1677	3.2/2.9/2.7	horizontal	0.92974	39/6
Roháčska	ROH-1	49.211154	19.749687	1418	2.0/1.4/0.8	178/16	0.98653	52/7
	ROH-2	49.211242	19.749856	1414	2.0/1.5/0.9	105/25	0.98646	53/7
	ROH-3	49.211612	19.749911	1412	1.9/1.4/0.6	120/15	0.98941	53/7
	ROH-4	49.211602	19.749830	1409	1.9/1.2/0.8	310/12	0.98818	53/7
Smutna	SMU-1	49.200121	19.741379	1724	2.0/1.4/0.8	205/8	0.95770	54/7
	SMU-2	49.200201	19.741316	1738	2.6/2.0/1.1	25/12	0.96283	54/7
	SMU-3	49.200249	19.740301	1752	1.9/3.0/1.0	150/4	0.94848	54/7
	SMU-4	49.200228	19.740171	1756	2.7/1.9/1.9	15/19	0.95856	54/7
Spálena-Lower	SPA-1	49.207499	19.725761	1495	4.9/4.2/1.5	195/11	0.98918	42/6
	SPA-2	49.207453	19.726210	1519	4.3/2.9/1.6	190/2	0.98907	43/6
	SPA-3	49.207574	19.725881	1530	7.1/4.3/2.8	225/9	0.98900	44/6
	SPA-4	49.209057	19.728034	1488	6.9/6.3/3.3	80/11	0.99025	42/6
	SPA-5	49.209283	19.727911	1487	1.9/1.3/1.0	250/7	0.99155	42/6
	SPA-6	49.209300	19.727963	1490	2.2/1.8/1.3	180/23	0.99155	42/6
Spálena-Middle	SPA-10	49.203861	19.714079	1753	7.9/5.7/4.0	270/7	0.98865	53/7
	SPA-11	49.203905	19.714053	1752	6.7/4.6/2.2	25/6	0.98865	53/7
	SPA-12	49.204510	19.715366	1730	8.7/6.3/4.7	285/8	0.99004	52/7
Spálena-Upper	SPA-7	49.202105	19.708552	1867	4.7/3.3/1.5	60/16	0.98208	58/7
	SPA-8	49.202283	19.708459	1870	3.8/2.6/1.8	185/5	0.97899	58/7
	SPA-9	49.202324	19.708682	1865	3.0/2.8/1.5	horizontal	0.98119	58/7
Žiarska	ZlA-1	49.192925	19.735390	1778	1.9/1.8/1.3	215/6	0.96119	54/7
	ZlA-2	49.192764	19.735595	1779	3.3/2.4/1.5	95/7	0.97711	54/7
	ZlA-3	49.192787	19.736714	1775	2.2/2.2/1.7	145/17	0.97672	55/7

ZlA-4	49.192514	19.736823	1776	4.7/2.3/1.6	310/7	0.97189	55/7
ZlA-5	49.192598	19.736127	1774	4.5/3.8/3.7	150/5	0.97455	54/7